

MICROSTRUCTURAL EVOLUTION IN ADIABATIC SHEAR LOCALIZATION IN STAINLESS STEEL

M. A. Meyers[†], M. T. Perez-Prado[†], Q. Xue[†], Y. Xu[‡], and T. R. McNelley^{*}

[†] *University of California, San Diego, La Jolla, CA, 92093*

[‡] *Institute of Metals Research, CAS, China*

^{*} *Naval Postgraduate School, Monterey, CA*

Abstract: Shear bands were generated under prescribed and controlled conditions in stainless steel (Fe-18%Cr-8%Ni). Hat-shaped specimens, deformed in a Hopkinson bar were used, yielding strain rates of approximately 104s⁻¹ and shear strains that could be varied between 1 and 100. Specimens recovered from the collapse of thick-walled cylinders were also investigated. Microstructural characterization was performed by electron backscattered diffraction (EBSD) with orientation imaging microscopy (OIM), and transmission electron microscopy (TEM). The shear-band thickness was approximately 8 μm . This low-stacking fault energy alloy deforms, at the imposed strain rates (outside of the shear band), by planar dislocations and stacking fault packets, twinning, and occasional martensitic phase transformations at twin-twin intersections. EBSD reveals gradual lattice rotations of the grains approaching the core of the band. A [110] fiber texture (with the [110] direction perpendicular to both shear direction and shear plane normal) develops both within the shear band and in the adjacent grains. The formation of this texture, under an imposed global simple shear, suggests that rotations take place concurrently with the shearing deformation. This can be explained by compatibility requirements between neighboring deforming regions. EBSD could not reveal the deformation features at large strains because their scale was below the resolution of this technique. Transmission electron microscopy reveals a number of features that are interpreted in terms of the mechanisms of deformation and recovery/recrystallization postulated. They include the observation of grains with sizes in the nanocrystalline domain. The microstructural changes are described by an evolutionary model, leading from the initial grain size of 15 μm to the final submicronic (sub)grain size. Calculations are performed on the rotations of grain boundaries by grain-boundary diffusion, which is 3 orders of magnitude higher than bulk diffusion at the deformation temperatures. They indicate that the microstructural reorganization can take place within the deformation times of a few milliseconds.

INTRODUCTION

The characterization of post-deformation microstructures within shear bands is a very important tool in the development of our understanding of the thermo-mechanical evolution during shear localization. The eternal question of the correlation of the post deformation structure with the one evolving during deformation will always persist. Nevertheless, significant progress has been made and a number of structural alterations have been either suggested or demonstrated: recovery, recrystallization (both

dynamic and static), phase transformations, comminution (of brittle materials), amorphization, and crystallization. The arsenal of the modern Materials Scientist has recently gained the addition of a powerful new technique, Electron Backscattering Scanning Microscopy. This method, in combination with transmission electron microscopy is helping the elucidation of the deformation/recovery mechanisms.

EXPERIMENTAL TECHNIQUES

Shear bands were generated in the AISI 304 stainless steel by two methods:

(a) the explosive collapse of a thick-walled cylinder under controlled and prescribed conditions; this technique was developed by Nesterenko and Bondar[1] and applied to stainless steel by Xue et al.[2].

(b) the hat-shaped specimen method, using a split Hopkinson bar in the compression mode to generate large shear strains in a small region (~200 μm thick). This method has been successfully used to generate shear localization regions in a number of metals (e.g., Andrade et al.[3]).

In the first case, the bands form freely, initiating at the internal surface of the cylinder. In the latter case, they are forced to form by the high localized shear strains.

The characterization methods used were transmission electron microscopy and orientation imaging microscopy by backscattered electron diffraction. Whereas TEM has been employed to characterize shear bands for twenty years (Ti, Al-Li, Cu, Ta, stainless steel[4], ferritic steels, etc), EBSD is a new addition to the arsenal of characterization techniques. It enables the identification of the crystallographic orientation on a sub-micron scale. An entire map of orientations can be obtained by this technique and the lattice rotations associated with plastic deformation can be followed.

The specimens for TEM were prepared by sectioning the thick-walled cylinders in a high-speed diamond saw, followed by mechanical polishing to a thickness of 150 μm and electropolishing in a solution of 10% HNO_3 in methanol. The specimens for EBSD were taken from hat-shaped specimens sectioned parallel to the cylinder axis and mechanically polished.

TRANSMISSION ELECTRON MICROSCOPY

The AISI 304 stainless steel exhibited, outside of the shear band, the structure characteristic of high-strain rate deformation which had been systematically identified earlier by Staudhammer et al.[6]. It is characterized by twins and stacking faults, propitiated by the low stacking-fault energy of 304 SS ($\gamma = \text{J/m}^2$). Figure 1(a) shows such a structure composed of intersecting twins; the foil orientation is close to $[100]$, providing a perpendicular pattern of twins, which are on $\{111\}$. In Figure 1(b) a localized deformation band is shown, distorting then twins. Another very interesting feature observed was the α martensite

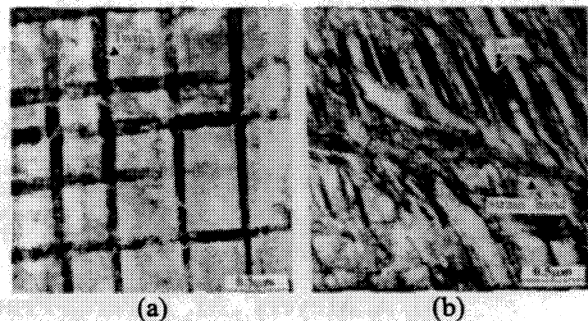


Figure 1. (a) Deformation twins; (b) Microshear band intersecting and deforming twins.

which nucleated in the strain bands, particularly at the intersections between twins and bands. Figure 2 shows an example; the presence of martensite could be confirmed by dark-field analysis; the dark-field image through the appropriate martensite spot is shown in Figure 2(b). Essentially, these results confirm earlier investigations[6].

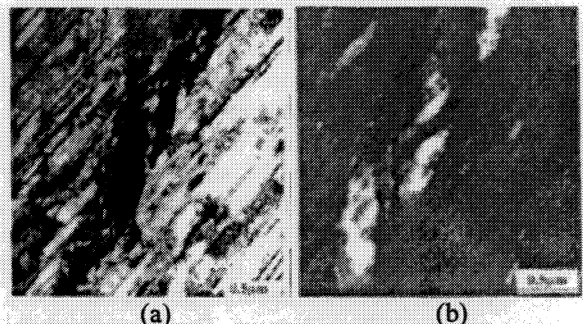


Figure 2. Martensite laths in deformed lattice (a) BF; (b) DF.

The microstructure inside of the shear band was radically different. Two principal domains could be identified:

(a) A region composed of nanoscale grains. Figure 3 shows this region. Figure 4 shows a dark field TEM micrograph. The grains are approximately 100-200 nm in diameter. These grains have clear boundaries and are equiaxed. This structure is similar to the ones observed in titanium[7], copper[4], Al-Li[8], and brass[9]. It has been attributed to a rotational recrystallization mechanism, which is quantitatively expressed by Meyers et al.[10,11]. Mataya, Carr, and Krauss[5] were the first to analyze shear bands in stainless steel

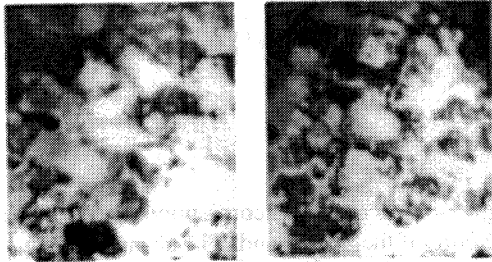


Figure 3. Microcrystalline structure (d~100-200nm) inside bands.



Figure 4. Dark field of nanocrystalline region.

and the y correctly identified the mechanism for the formation of these grains.

- (b) A glassy region, separated from the nanocrystalline region by an interface. Figure 5 shows this interface, with the glassy region at the right and the crystalline one at the left. High resolution transmission electron microscopy confirms the amorphous nature of the material. This is a surprising finding and the first observation of a crystalline to amorphous transition in a shear band. Barbee et al.[10] were able to produce the amorphous transition

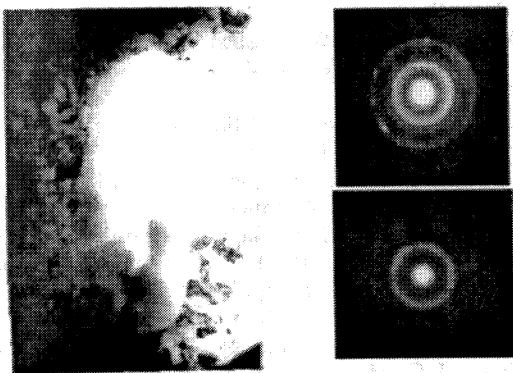


Figure .5 Interface between nanocrystalline and amorphous regions.



Figure 6. High-resolution TEM of amorphous region.

in 304 SS by sputter depositing it. However, this was only possible for a carbon concentration greater than 5 at. %.

Figure 7 illustrates the microtexture of the grains adjacent to the shear band. The regions colored in white in the Orientation Imaging Map (OIM) in the center are highly deformed areas, from where no orientation data could be acquired. The shear band is located at the center of the OIM map. The shear direction (SD) is parallel to the vertical direction in the map, and the shear plane normal (SPN) is parallel to the horizontal direction. Grain subdivision on approaching the shear band can be clearly appreciated. Grains subdivide in order to be able to accommodate the imposed shear strain. Lattice rotation has been followed along several paths in the microstructure, depicted in Figs. 7a, 7b, and 7c. The lattice rotation within a (sub)grain (not subdivided) is only small (Fig. 7a), whereas significant lattice rotations can be observed along several (sub)grains (Fig. 7b) that initially belonged to the same grain. In addition to accommodating the imposed shear strain, neighboring grains must also deform in a compatible fashion. Figure 7c shows the microtexture along a path that comprises several adjacent grains. A fiber texture is formed, in which the fiber axis, close to the $\langle 110 \rangle$ direction, is parallel to both the shear direction and the shear plane normal. Fiber textures also form during tensile deformation of polycrystals due to the need of achieving compatible deformation between neighboring grains [Taylor, Pérez-Prado et al.].

Figure 8 shows the microtexture data corresponding to the core of the shear band. Orientation data could only be acquired in isolated

locations (see figure 7). The spatial resolution of the EBSD technique is about $0.3\ \mu\text{m}$, and therefore the absence of data in larger regions of the shear band indicates that the scale of the microstructure is smaller than the resolution limit. It is interesting to note that again a fiber texture is formed. The fiber is not perfect since only limited information is available in this region. This is a deformation texture, similar to that obtained in the grains

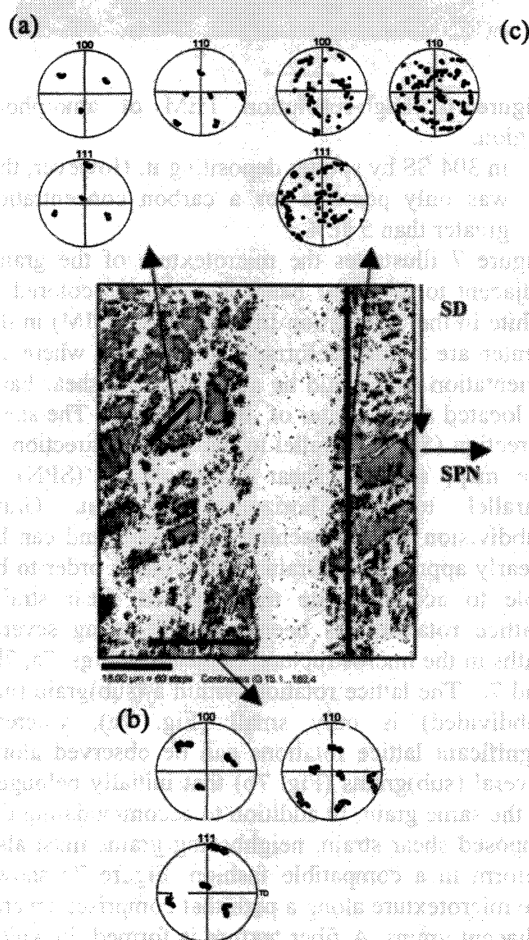


Figure 7. Microtexture data corresponding to regions adjacent to the shear band. (111), (110), and (100) pole figures showing (a) the lattice rotation within a (sub)grain, (b) the lattice rotation along a subdivided grain, and (c) the microtexture of several adjacent grains. The shear direction (SD) is the vertical and the shear plane normal (SPD) is the horizontal.

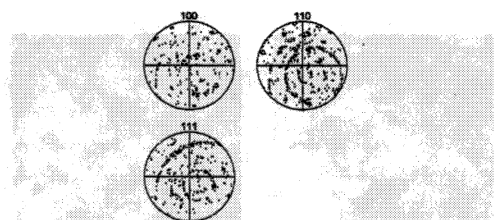


Figure 8. Microtexture corresponding to regions in the core of the shear band. The shear direction (SD) is the vertical and the shear plane normal (SPN) is the horizontal.

adjacent to the band. This indicates that grain subdivision continues to take place within the band, with the aim of accommodating the imposed shear strain and maintaining neighboring grain compatibility. (Research supported by US Army Research Office MURI Program under Contract DAAH04-96-1-0376 and the Department of Energy Grant DEFG0300SF2202).

REFERENCES

1. Nesterenko, V. F., and Bondar, M. P., *DYMAT* J., 1,243-251(1994).
2. Xue Q., Nesterenko, V. F., and Meyers, M. A., in *Shock Compression of Condensed Matter-1999*, AIP, 2000, 431-434.
3. Meyer, L. W., and Manwaring, S., in *Metallurgical Applications of Shock-Wave and High-Strain-Rate Phenomena*, M. Dekker, 1986, pp. 657-674.
4. Andrade, U. R., Meyers, M. A., Vecchio, K. S., and Chokshi, A. H., *Acta Met.*, 42,3183-3195(1994).
5. Mataya, M. C., Carr, M. J., and Krauss, Met. Trans. 133A, 1263-1274(1982).
6. Staudhammer, K. P., Frantz, C. E., Hecker, S., S., and Murr, L. E., in *Shock Waves and High-Strain Rate Phenomena in Metals*, M. Dekker, 1981, pp.91-112.
7. Meyers, M. A., and Pak, H.-r., *Acta Met.*, 34, 2493(1986).
8. Xu, Y. B., Zhong, W. L., Chen, Y. J., Shen, L. T., Liu, Q., Bai, Y. L. and Meyers, M. A., *Mat. Sci. Eng.*, A299, 287-295(2001).
9. Li, Q., Xu, Y. B., Lai, Z. H., Shen, L. T., and Bai, Y. L., *Mat. Sci. Eng.*, A276, 127(2000).
10. Barbee, T. J. Jr., Jacobson, B. E., and Keith, D. L., *Thin Solid Films*, 63, 143-150(1979).
11. Meyers, M. A., LaSalvia, J. C., Nesterenko, V.F., Chen, Y. J., Kad, B. K., *Proc. 3rd Intl. Conf. Recrystallization and Related Phenomena*, (REX'960t. Mcnolley, Ed., P. 279.
12. Meyers, M. A., Xue, Q., Nesterenko, V. F., LaSalvia, J. C., *Mat. Sci. Eng.*, in press(2001).